Received: 22 January 2020 | Accepted: 24 July 2020

DOI: 10.1002/jcp.29998

ORIGINAL RESEARCH ARTICLE

Journal of Cellular Physiology WILEY

Effects of photoperiod on morphology and function in testis and epididymis of *Cricetulus barabensis*

Junjie Mou | **Jinhui Xu** | **Zhe Wang** | **Chuanli Wang** | **Xueqi Yang** | **Xingchen Wang** | **Huiliang Xue** | **Ming Wu** | **Laixiang Xu**

College of Life Sciences, Qufu Normal University, Qufu, Shandong, China

Correspondence
Laixiang Xu, College of Life Sciences, Qufu Normal University, 57 Jingxuan East Road, Qufu, 273165 Shandong, China.
Email: xulx@qfnu.edu.cn

Funding information
National Natural Science Foundation of China, Grant/Award Numbers: 31670385, 31770455, 31800308, 31972283

Abstract

Photoperiod regulates the seasonal reproductive rhythms of mammals by influencing the development and function of sexual organs; however, the underlying mechanism remains unclear. We examined the morphology and functioning of the main sex organs of striped dwarf hamsters (*Cricetulus barabensis*) under different photoperiods (short daylight [SD], moderate daylight [MD], and long daylight [LD]) and further investigated the underlying molecular mechanisms. There was an inverse correlation between blood melatonin levels and photoperiod in the order SD > MD > LD. Decreases in body and tissue weights were observed under SD, whereas testis and epididymis weights between MD and LD were comparable. The diameters of the spermatogenic tubules, thickness of the spermatogenic epithelium, and the number of spermatogonia and Sertoli cells decreased under SD, whereas the serum-luteinizing hormone, follicle-stimulating hormone, and fecal testosterone concentrations decreased under LD. In SD, bax/bcl2 protein expression increased in the testes and decreased in the epididymides, whereas LC3II/LC3I remained unchanged in the testes and increased in the epididymides compared with the MD group. In LD, bax/bcl2 and LC3II/LC3I protein expression levels were unchanged in the testes but were decreased in the epididymides. In SD and LD, adenosine triphosphate synthase and citrate synthase protein expression levels were unchanged in the testes but were decreased in the epididymides. Drp1 and Mff protein expression increased in the testes and decreased in the epididymides. Overall, different regulatory mechanisms in the testis and epididymis led to degeneration under SD and maintenance under LD, preferentially protecting mitochondrial function in the testis by regulating mitochondrial fission.

KEYWORDS

apoptosis, autophagy, *Cricetulus barabensis* , mitochondria, photoperiod

1 | INTRODUCTION

Seasonal breeders inhibit their own reproductive behavior by reducing testis weight and volume and by lowering sperm and spermatocyte production during the nonreproductive season. Photoperiod is one of the most important factors affecting seasonal reproductive behavior (Han et al., 2017; Lewis, 2006; Pieri et al., 2014). Several studies have shown that seasonal rhythm mammals regulate

Junjie Mou, Jinhui Xu, and Zhe Wang contributed equally to this work.

reproductive rhythms via the hypothalamus-pituitary-gonadal axis through melatonin secretion by photosensitive organs such as the pineal gland (Kelestimur et al., 2012; Shi, Li, Bo, & Xu, 2013). Current studies on seasonal reproductive rhythms in mammals, such as white-footed mice (*Peromyscus leucopus*), bank voles (*Myodes glareolus*), Djungarian hamsters (*Phodopus sungorus*), and Syrian hamsters (*Mesocricetus auratus*), have shown that short-light stimulation induces testicular degeneration, mainly by reducing weight and volume (Bonda-Ostaszewska & Wlostowski, 2015; Furuta et al., 1994; Martinez-Hernandez et al., 2018; Young & Nelson, 2001). Testicular atrophy in golden hamsters (*M. auratus*) under short daylight exposure is usually accompanied by decreases in serum luteinizing hormone (LH), follicle-stimulating hormone (FSH), and testosterone (TTE; Console et al., 2002; Kawazu et al., 2003), whereas long daylight exposure increases serum LH and FSH levels (Turek, Elliott, Alvis, & Menaker, 1975). Therefore, testicular degeneration caused by photoperiodic variation may involve changes in morphology, secretion, and spermatogenic function.

The balance between autophagy and apoptosis is one of the key factors for maintaining tissue morphology and quality (Campbell & Quadrilatero, 2016; C. Wang et al., 2017), and the application of short daylight results in an increase in DNA fragmentation in Syrian hamsters (Morales et al., 2002; Seco-Rovira et al., 2014). This may involve the mitochondrial–nuclear apoptosis pathway that is initiated by bax and inhibited by bcl2, in which caspase 3 is the main effector (Antonsson et al., 1997; Manickam, Kaushik, Karunakaran, & Bhansali, 2017). Study of the South American plains vizcacha (*Lagostomus maximus*) demonstrated that the immunolocalization of microtubule-associated protein 1 light chain 3 (LC3) and beclin-1 (BECN1) in the inactive testes stops in July (similar to short photoperiod), meaning that the level of autophagy decreases (González, Isla, & Vitullo, 2018). LC3 is the key factor in the initiation of autophagy (Schaaf, Keulers, Vooijs, & Rouschop, 2016). Meanwhile, BECN1 is an important promoter of autophagy, and mammalian target of rapamycin (mTOR) plays an inhibitory role in autophagy (Mariño, Niso-Santano, Baehrecke, & Kroemer, 2014). However, most of the studies on the mechanisms of autophagy and apoptosis have focused on seasonal changes, whereas studies concerning photoperiod are limited, and there are few reports concerning the related mechanisms.

Furthermore, long daylight exposure also promotes mitochondrial density in the testes of rats and bank voles, whereas the number of mitochondria decreases with short daylight exposure (Kus et al., 2004; Tahka, 1988). This may involve mitochondrial fission. Drp1 is the most important factor in mitochondrial division, and Mff promotes the activity of Drp1 variation (Fekkes, Shepard, & Yaffe, 2000), while Fis1 inhibits mitochondrial division (Liu & Chan, 2015). Mitochondria are responsible for aerobic oxidation and energy supply, and citrate synthase (CS) and adenosine triphosphate (ATP) synthase are their rate-limiting enzymes (Danson & Hough, 2001; Kramarova et al., 2008). Investigating the above indicators can assess changes and elucidate related variation in the mechanisms of mitochondrial function under different photoperiods.

The above suggests that during various photoperiods, the structure and function of the testes, which is the basic parameter for measuring the reproductive capacity of small mammals, may be closely related to apoptosis, autophagy, and mitochondrial function (Bonda-Ostaszewska & Wlostowski, 2015; Furuta et al., 1994; Young & Nelson, 2001). However, investigations of the mechanisms underlying these changes have mainly involved Syrian hamsters that hibernate in winter, and changes in their bodies under photoperiod treatment are quite different from those of other hamsters (Bartke & Parkening, 1981; Mauer & Bartness, 1994; Tups et al., 2006; D. L. Xu & Hu, 2017). In addition, these studies have not examined accessory reproductive organs such as the epididymis. The striped dwarf hamster (*Cricetulus barabensis*) is a small nonhibernating mammal that is widely distributed in the north temperate zone of Asia. Current studies have shown that there are significant seasonal changes in gene expression related to reproduction in the hypothalamus, testis, epididymis, ovary, and uterus (D.-L. Xu, Hu, & Tian, 2018; L. Xu, Xue, Li, Xu, & Chen, 2017; Z.-J. Zhao, Cao, Li, & Yu, 2010). In addition, striped dwarf hamsters do not hibernate in winter (Xue, Xu, Chen, & Xu, 2014), and whether this habit will cause short photoperiod to have a different effect on it than that of Syrian hamsters remains unclear. More important, the testis and epididymis of the striped dwarf hamsters account for a larger proportion of the body compared with Syrian hamsters and European hamsters (*Cricetus cricetus*); in this species, the testicles protrude from the abdominal cavity to the tail, forming a very obvious scrotum below the tail. However, the significance of this particular morphological feature to reproductive behavior remains unclear (Moore, 1965; Reznik, Reznik-Schuller, & Mohr, 1973; Yerganian, 1958).

Accordingly, the present study focused on the morphological and functional changes in the testis and epididymis of hamsters under different photoperiods and the underlying mechanisms. We hypothesized that photoperiod affects the morphology and function of reproductive organs in hamsters. We also postulated that changes in apoptotic and autophagic levels lead to this change. To test these hypotheses, we studied the morphological changes in the testes and epididymides (i.e., diameter of seminiferous tubules, numbers of Leydig cells, and Sertoli cells), the ultrastructural changes under electron microscopy, and the spermatogenesis (thickness of spermatogenic epithelium) and secretory function (FSH, LH, and TTE) of the testes in hamsters. On this basis, the effects of photoperiod on apoptosis (bax, bcl2, Cyto *C*, caspase 9, and caspase 3), autophagy (LC3I, LC3II, P62, BECN1, and mTOR), and mitochondria (ATP synthase, CS, Drp1, Mff, and Fis1) were studied to explore the mechanisms underlying different sex organs changes.

2 | MATERIALS AND METHODS

2.1 | Ethics statement

The Qufu Normal University Ethics Committee approved all of the procedures. Experiments followed the Laboratory Animal Guidelines

for the Ethical Review of Animal Welfare (GB/T 35892-2018) and were approved by the Animal Care and Use Committee of Qufu Normal University.

2.2 | Animals and groups

The striped dwarf hamsters (*C. barabensis*) were prepared in our laboratory as previously described (Xue et al., 2014; L. Zhao et al., 2014). Briefly, hamsters were caught in the Yinan Region in Shandong Province, China and were provided water and rat chow ad libitum. The striped dwarf hamsters were weighed, and 60 male individuals (20–40 g) were selected as samples. The hamsters were placed in a light controller for 12:12 hr of adaptive treatment at a temperature of 22 ± 2°C and relative humidity of 55 ± 5%, with a normal amount of food (3 g/d) and water.

After matching for body weight, the hamsters were randomly assigned into three groups: a long daylight group (LD) exposed to a long photoperiod (16 hr:8 hr; light from 04:00 to 20:00); a moderate daylight group (MD) exposed to a moderate photoperiod (12:12 hr; light from 06:00 to 18:00); and a short daylight (SD) group exposed to a short photoperiod (8:16 hr; light from 08:00 to 16:00). The light intensity was set at 150 ± 10 lx, and exposure time was 8 weeks.

2.3 | Sample preparation

At the end of the exposure, the animals were killed by CO_2 asphyxiation at 22:00 on the final day after all of the hamsters had been in the dark for at least 2 hr (Z. Wang, Xu, Mou, Kong, Wu, et al., 2020). Blood samples were immediately collected after sacrifice and stored at 4°C for 30 min, then centrifuged at 3,000 rpm for 15 min at 4°C. Serum MT, FSH, LH, and fecal TTE levels were estimated using an enzyme-linked immunosorbent assay Labsystems Multiskan MS 352 (Shanghai Hengyuan Biological Technology Co., Ltd., H-40277, Shanghai, China). Testis and epididymis were removed and weighed. The right testis or epididymis was cut into three parts; one part was immersed in paraformaldehyde-glutaraldehyde fixative for transmission electron microscopy (TEM), while the other two parts were immersed in 4% paraformaldehyde for paraffin and frozen section embedding. The left testis or epididymis was stored in a refrigerator at −80°C for subsequent western blot experiments.

2.4 | Histological studies

Hematoxylin-eosin staining (H&E staining) was performed to assess changes in cellular morphology. The tissues were embedded in paraffin blocks. Serial sections (5-μm thickness) of the entire tissue were prepared. After rehydration, the sections were stained with hematoxylin for 30 min, then slowly rinsed with running water for at least 15 min. The slices were separated in 1% hydrochloric acid-alcohol solution for 15 s, then slowly rinsed with running water for at least 5 min. The sections were dyed with eosin for 5 min and then rinsed with running water for 15 min. The slides were then dried, mounted with neutral gum, and sealed. The sections were examined under a microscope (Olympus, BX51, Japan). We analyzed 10 samples in each group, six images from each sample, and six seminiferous tubules in each image. When selecting the seminiferous tubules, the length of the major axis was at most 1.5 times that of the minor axis. In the IPP 6.0 analysis, the diameter (mean) and spermatogenic epithelial thickness of individual tubules were calculated after the scale was calibrated. To determine how the diameters of testicular seminiferous tubules and the thickness of the seminiferous epithelium changed, the number of spermatogonia and Sertoli cells in the seminiferous tubules were determined by counting the nuclei of spermatogonia and nucleoli of Sertoli cells. In addition, we calculated the number of cells per unit area according to the area formula after counting all Leydig cells per image (Ansari et al., 2018; Costa, Menezes, & Paula, 2007).

2.5 | TEM studies

The tissues of each group were cut into blocks and immersed in 3% glutaraldehyde–paraformaldehyde for TEM, dehydrated with a graded series of ethanol, and embedded in epoxy resin. TEM evaluation was performed as previously described (Z. Wang et al., 2019; Zhe Wang et al., 2020). Semithin sections of the tissue samples were prepared and stained with methylene blue (Biazik, Vihinen, Anwar, Jokitalo, & Eskelinen, 2015). The sections were adjusted under a microscope and sliced with an ultramicrotome (LKB-NOVA). The ultrathin sections were double-stained with Reynolds' lead citrate and ethanolic uranyl acetate. The sections were examined with a transmission electron microscope (JEOL, JEM-100SX, Japan), and images were processed with IPP 6.0 software. Images were analyzed using the measurement tools provided by this software.

2.6 | Immunohistochemistry analysis

The testis and epididymis were fixed in 4% paraformaldehyde for 24 hr, dehydrated across a sucrose gradient (10%, 20%, and 30%), washed with 100% acetone, and embedded in an optimal cutting temperature compound (Sakura, MA). We cut 10-μm-thick frozen testis and epididymis cross-sections from the mid-belly of each tissue at −20°C using a cryostat (Leica, Wetzlar, CM1850, Germany). After air-drying for 2 hr, 10 sections from each tissue were randomly selected for follow-up experiments. Sections were washed with phosphate-buffered saline (PBS), then permeabilized with 0.2% Triton X-100 in 0.1% sodium at 37°C for 30 min. Cleared sections were stained in blocking solution (5% bovine serum albumin [BSA]; Boster, Wuhan, China) for 10 min at room temperature and then with an anti-laminin rabbit polyclonal antibody (1:500, BA1761-1; Boster) solution at 4°C overnight. The following day, the sections were incubated with goat anti-rabbit Alexa Fluor 647 (1:200, #A21245;

Thermo Fisher Scientific, Rockford, IL) at 37°C for 2 hr. After this, the sections were incubated with rabbit anti-LC3 (1:200; Cell Signaling Technology [CST], Danvers, MA), rabbit anti-P62 (1:200; Proteintech, Wuhan, China), and goat anti-rabbit Alexa Fluor 488 (1:200, #A11034; Thermo Fisher Scientific) under the same conditions. Finally, the glass slides were placed in 4′,6-diamidino-2-phenylindole (DAPI; 1:100, #D9542; Sigma-Aldrich) at 37°C for 30 min. Images were visualized using a confocal laser scanning microscope by krypton/argon laser illumination at wavelengths of 350, 488, and 647 nm emitted light and captured at 461, 526, and 665 nm. The number of protein aggregates of LC3 and P62 were counted by selecting an area with dimensions of 100 μm × 100 μm.

2.7 | Terminal deoxynucleotidyl transferase biotin-dUTP nick end-labeling (TUNEL) staining

DNA fragmentation induced by apoptosis was determined by double-labeled fluorometric TUNEL detection, and evaluation was done as previously described (Fu et al., 2016). Briefly, 10-μm-thick frozen tissue cross-sections were air-dried and fixed in 4% paraformaldehyde in PBS (pH 7.4) at room temperature for 20 min. Then, the sections were permeabilized with 0.2% Triton X-100 in 0.1% sodium citrate at 4°C for 2 min and incubated with an anti-laminin rabbit polyclonal antibody (1:500; Boster) at 4°C overnight. After washing with PBS for 30 min, the sections were incubated with the fluorochrome-conjugated secondary AF647 antibodies at room temperature for 2 hr. Subsequently, TUNEL (#MK1023; Boster) reaction mix was added at the recommended 1:9 ratio, and the sections were incubated for 60 min at 37°C in a humidified chamber in the dark according to the manufacturer's protocol. Finally, the sections were counterstained with DAPI. Both positive and negative controls were included in each experiment. Sections were treated with DNase I (Tiangen, Beijing, China) in DNase buffer for 10 min at room temperature before incubating with the anti-laminin rabbit polyclonal antibody as positive controls, and then incubated without the TdT enzyme as the negative control. Images were visualized using a confocal laser scanning microscope (Olympus, Osaka, Japan) at an objective magnification of ×40.

2.8 | Western blot analysis

Western blot evaluation was performed as previously described (Z. Wang et al., 2019). Total protein was extracted and solubilized in sample buffer (100 mM Tris [pH 6.8], 5% 2-β-mercaptoethanol, 5% glycerol, 4% sodium dodecyl sulfate (SDS), and bromophenol blue) with the extracts of the testis and epididymis protein and then resolved via SDS-polyacrylamide gel electrophoresis (10% Laemmli gel with an acrylamide/bisacrylamide ratio of 29:1% and 98% 2,2,2-trichloroethanol; Aladdin, JI522028, China). For electrophoresis, two identical gels for sample sequence and protein quantification were used. One plate was used for total protein quantification as an internal reference, and the other plate was employed for follow-up target protein quantification. After electrophoresis, the proteins were electrically transferred onto polyvinylidene fluoride membranes (0.45-μm pore size) using a Bio-Rad semi-dry transfer apparatus. The blotted membranes were blocked with 1% BSA in Tris-buffered saline (TBS; 150 mM NaCl, 50 mM Tris-HCl, pH 7.5) and incubated with rabbit anti-LC3 (1:1,000), rabbit anti-P62 (1:1,000), rabbit anti-BECN1 (1:1,000, #11306; Proteintech), rabbit anti-mTOR (1:1,000, #20657; Proteintech), rabbit anti-bax (1:1,000, #50599; Proteintech), rabbit anti-bcl2 (1:1,000, #3498S; CST), rabbit anti-Cyto *C* (1:1,000, #11940; CST), rabbit anti-caspase 3 (1:1,000, #19677; Proteintech), rabbit anti-caspase 9 (1:1,000, #10380; Proteintech), rabbit anti-Drp1 (1:1,000, #12957; Proteintech), rabbit anti-Mff (1:1,000, #17090; Proteintech), rabbit anti-Fis1 (1:1,000, #10956; Proteintech), rabbit anti-ATP synthase (1:1,000, #14676; Proteintech), rabbit anti-citrate synthase (1:1,000, #16131; Proteintech), and rabbit anti-β-actin (1:5,000, #20536; Proteintech) in TBS containing 0.1% BSA at 4°C overnight. The membranes were then incubated with IRDye 800 CW goat anti-rabbit secondary antibodies (1:5,000, #31460; Thermo Fisher Scientific) for 90 min at room temperature and visualized with an Odyssey scanner (LI-COR Biosciences, Lincoln, NE; Yang, He, Gao, Wang, & Goswami, 2014). Quantification analysis of the blots was performed using ImageJ software. The immunoblot band density of each individual lane was standardized against the summed densities of the total proteins.

2.9 | Statistical analyses

SPSS version 22.0 was used for all of the statistical analyses. The data are presented as the mean ± *SD*. One-way analysis of variance (ANOVA) was used to determine the overall differences; Fisher's least significant difference (LSD) post hoc test was used to determine group differences. An ANOVA-Dunnett's T3 method was used when no homogeneity was detected. The results were deemed statistically significant at $p < .05$.

3 | RESULTS

3.1 | Hamster body weight (BW), tissue wet weight (TWW), and the ratio of tissue wet weight to body weight (TWW/BW)

The BW of hamsters did not significantly differ among the three groups before the experiment. After 2 months of treatment using different photoperiods, the BWs of the hamsters in the SD and LD groups had decreased by 4.3% ($p = .443$) and 3.4% ($p = .518$), respectively, compared with that before the experiment. In contrast, BW increased by 2.4% ($p = .685$) in the MD group compared with that before the experiment. Meanwhile, the BW after treatment in the SD group was significantly decreased compared with the MD group ($p < .05$). The TWW of the testes in the SD group was significantly

decreased compared with the MD and LD groups ($p < .05$), and the TWW of the epididymides in the SD group was significantly decreased compared with the MD and LD groups ($p < .05$). The TWW/BW of the testes and epididymides both showed that the ratio of the SD group was significantly decreased compared with the MD group ($p < .05$; Table 1).

3.2 | Blood MT, FSH, LH, and fecal TTE levels under different photoperiods

MT directly reflects the effects of photoperiod on an organism. Here, serum MT levels were increased in the SD group compared with the MD and LD groups ($p < .05$; Figure 1a). Serum LH and FSH levels were decreased in the LD group as compared with the SD and MD groups ($p < .05$; Figure 1b,c). Fecal TTE levels decreased with increasing illumination duration (Figure 1d).

3.3 | Morphological comparison of the testes and epididymides

Figure 2 shows tissue sections of the testes and epididymides stained with H&E. The seminiferous tubules were distinct and intact in the testes, with normal Leydig cells, Sertoli cells, spermatogonia, and mature and immature sperm (Figure 2a,b). The internal morphology of the epididymides was similar to that of the testes. The twisted and coiled vas deferens were observed in the epididymides, with epididymal epithelial cells in neat rows (Figure 2c,d).

The average seminiferous tubule diameter was lower in the testes of the SD group compared with the MD and LD groups ($p < .05$; Figure 3b). The number of spermatogonia in a single tubule showed the trend SD < LD < MD ($p < .05$; Figure 3c). In addition, the number of Sertoli cells per single tubule cross-section also decreased in the SD group compared with the MD and LD groups ($p < .05$; Figure 3d).

The thickness of the spermatogenic epithelium was decreased in the SD and LD groups compared with the MD group ($p < .05$; Figure 4b). In addition, the number of Leydig cells in the testis cross-sections of the SD group increased compared with the MD and LD groups ($p < .01$; Figure 4c).

3.4 | Ultrastructural changes in the nuclei and mitochondria of the testes and epididymides

A large number of germ cells and spermatids at different stages were observed in the testes that were subjected to three different photoperiods. In the testes of the SD and LD groups, the nuclei showed chromatin condensation, whereas in the epididymides of the SD and MD groups, the nuclei were deformed; the nuclear membranes exhibited severe contraction, and the chromatin had condensed. The nuclei of spermatogonia in the MD group of testes and the epididymides of the LD group appeared normal, with clear nuclear membranes and uniformly distributed chromatin (Figure 5).

The mitochondria of the testes and epididymides were irregularly oval; in the testes of the SD group, a reduction in mitochondrial cristae was observed. In the other groups, numerous cristae were clearly visible; the membranes were complete, and no significant structural changes were detected (Figure 6).

3.5 | DNA fragmentation

TUNEL staining provided direct evidence of apoptosis (Figure 7). DNA fragmentation as represented by green fluorescence was observed in the testes of the SD and LD groups in several adjacent cells, and blue fluorescence indicated the nuclei; these were hardly observed in the MD group. This result indicated that the apoptosis level of the testes was significantly increased in the SD and LD groups compared with the MD group (Figure 7a). The epididymides of the three groups showed few signs of DNA fragmentation (Figure 7b).

3.6 | Changes in LC3 and P62 puncta in the testes and epididymides under different photoperiods

The conversion of LC3I to LC3II is represented by the number of cytoplasmic LC3 puncta. Representative figures of LC3 immunofluorescence staining of the testes are shown in Figure 8a. The number of LC3 puncta in the testes did not significantly differ among the three groups, whereas the numbers of LC3 puncta in the epididymides of the SD and LD groups were increased compared with the MD group (Figure 8c).

TABLE 1 Effects of photoperiod on BW, TWW, and the ratio of TWW/BW in striped hamsters

			TWW at experiment time (g)		TWW/BW at experiment time (g/g)	
Groups	BW before photoperiod (g)	BW at experiment time (g)	Testis	Epididymis	Testis	Epididymis
SD	30.00 ± 1.63	28.70 ± 1.62	1.58 ± 0.14	1.65 ± 0.16	0.051 ± 0.001	0.053 ± 0.001
MD	29.60 ± 1.92	30.30 ± 1.68*	1.66 ± 0.10*	1.80 ± 0.24*	0.055 ± 0.001*	0.058 ± 0.002*
LD	30.66 ± 1.53	29.62 ± 1.55	1.71 ± 0.11*	1.75 ± 0.12*	0.057 ± 0.002*	0.058 ± 0.002*

Note: Data represent the mean ± standard deviation; $n = 10$.
Abbreviations: BW, body weight; LD, long daylight; MD, moderate daylight; SD, short daylight; SD, standard deviation; TWW, tissue wet weight.
*$p < .05$ relative to SD.

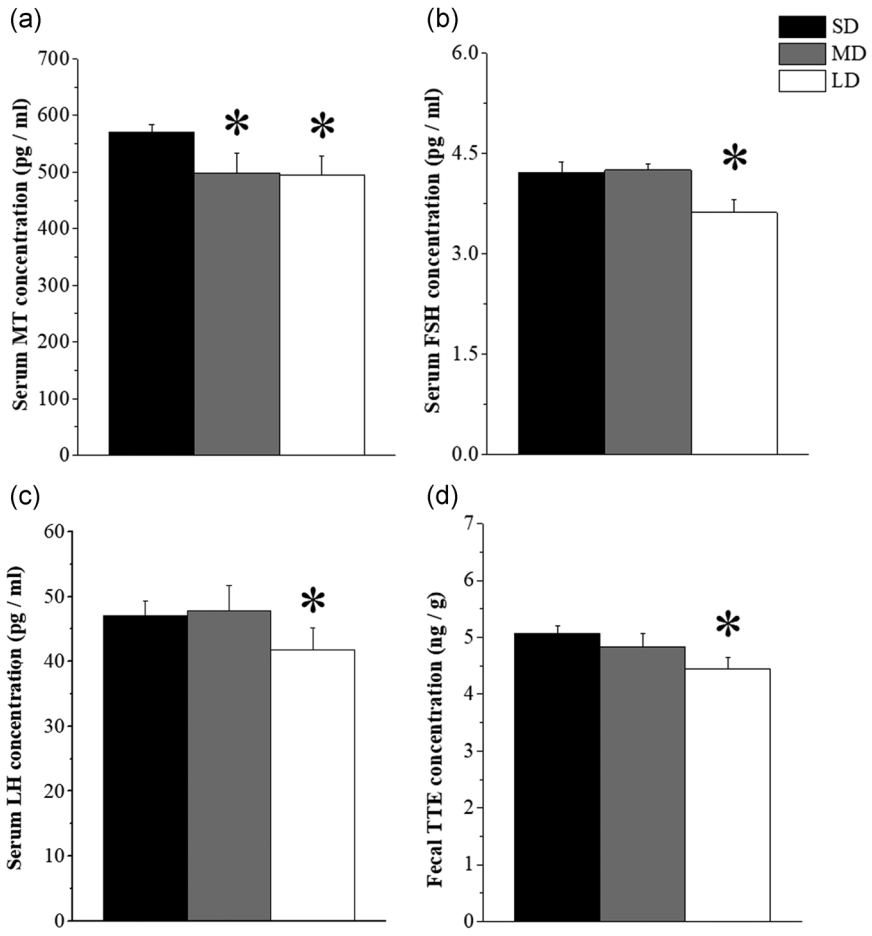

FIGURE 1 Hormones of MT, FSH, LH, and TTE in hamsters under three photoperiod conditions. (a) Serum MT levels in hamsters under three photoperiod conditions. (b) Serum LH levels in hamsters under three photoperiod conditions. (c) Serum LH levels in hamsters under three photoperiod conditions. (d) Fecal TTE levels in hamsters under three photoperiod conditions. Values are the means ± standard deviation, $n = 10$. FSH, follicle-stimulating hormone; LD, long daylight; LH, luteinizing hormone; MD, moderate daylight; SD, short daylight; TTE, testosterone. *$p < .05$ relative to SD

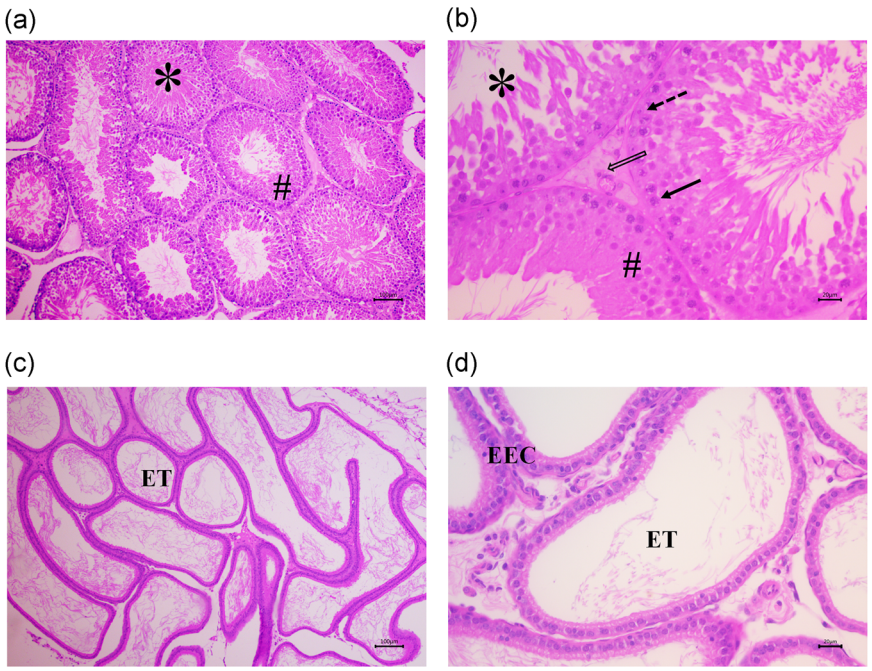

FIGURE 2 Histological structure of testis and epididymis in hamsters by HE staining. (a) Germ cells and seminiferous tubules of the testis are shown under low-power magnification. *seminiferous tubule; #seminiferous epithelium. Scale bar = 100 μm. (b) Seminiferous tubules of the testis are shown under high-power magnification. Solid arrow, spermatogonia; dotted arrow, Sertoli cells; hollow arrow, Leydig cells. Scale bar = 20 μm. (c) Seminiferous tubules in the epididymis are shown under low-power magnification. EEC, epididymal epithelial cells; ET, epididymis tubule; HE, hematoxylin and eosin. Scale bar = 100 μm. (d) Epididymal epithelial cells in the epididymis are shown under high-power magnification. Scale bar = 20 μm

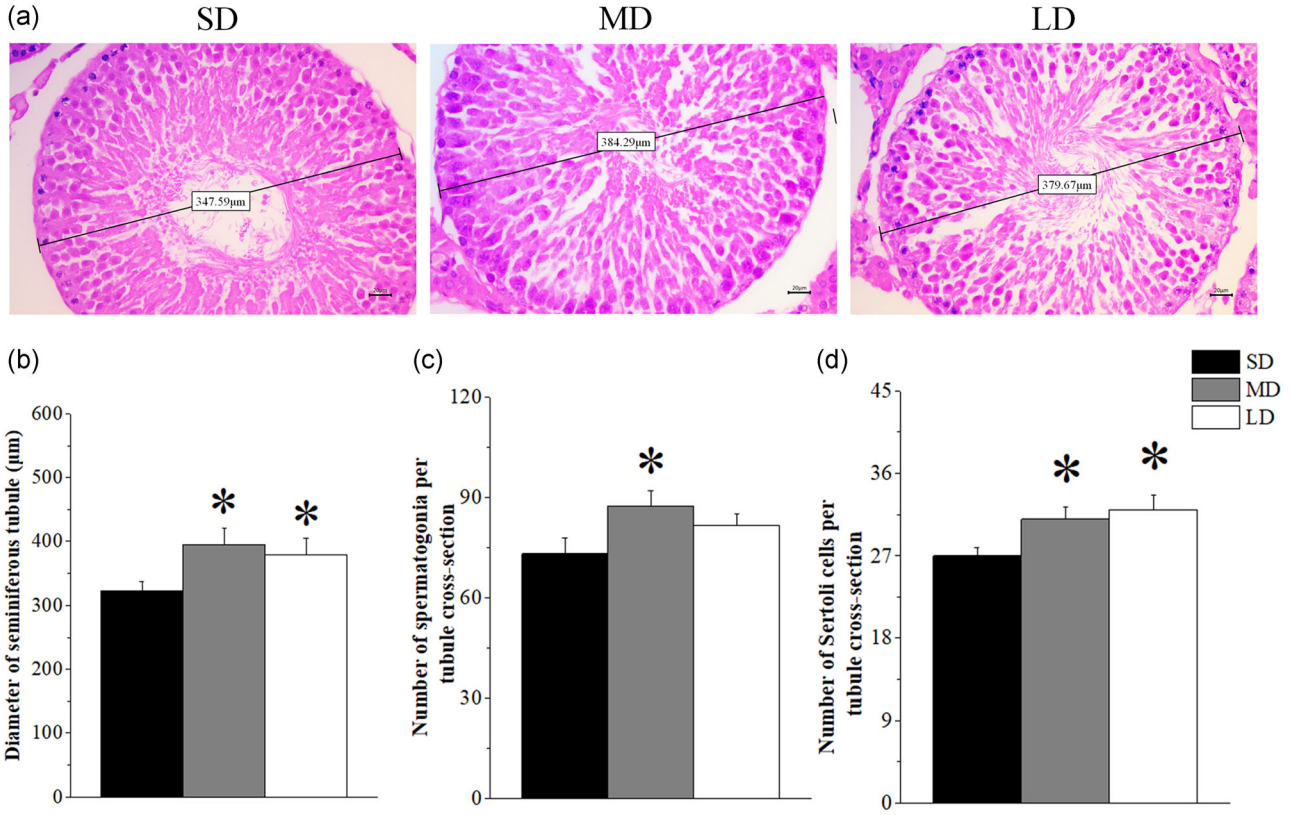

FIGURE 3 The diameter of the seminiferous tubules and the number of spermatogonia and sterile cells in the hamster by HE staining. (a) Seminiferous tubules from hamsters under three photoperiods showing diameters under higher-power magnification. Scale bar = 20 μm. (b) The diameters of the seminiferous tubules in the testes of hamsters under three photoperiods. (c) The number of spermatogonia per tubule cross-sections of hamster testes during three photoperiods. (d) The number of Sertoli cells per tubule in testis cross-sections of hamsters during three photoperiods. Sixty tubules were analyzed in each sample; 10 samples were analyzed in each group. Representative seminiferous tubule diameters measure 347.59, 384.29, and 379.67 μm during the SD, MD, and LD photoperiods, respectively. Values are the means ± standard deviation. $n = 10$. HE, hematoxylin and eosin; MD, moderate daylight; LD, long daylight; SD, short daylight. *$p < .05$ relative to SD

Representative images of P62 immunofluorescence staining are shown in Figure 8b, indicating that the number of P62 puncta in the testes increased in the LD and SD groups compared with the MD group, whereas in the epididymis, the number of P62 puncta decreased as follows: MD > LD > SD ($p < .05$; Figure 8d).

3.7 | Relative protein expression

The contents of bax, bcl2, Cyto *C*, caspase 3, and caspase 9 were detected by western blot analysis, as shown in Figure 9a.

Bax/bcl2 is one of the most important indicators of mitochondrial apoptosis. Bax/bcl2 and Cyto *C* protein expression in the testes were significantly increased in the SD group compared with the MD and LD groups ($p < .001$), whereas no significant difference was observed between the LD and MD groups (Figure 9d,e). In the epididymides, bax/bcl2 and Cyto *C* protein expression levels were the highest in the MD group ($p < .05$; Figure 9d,e).

Caspase 3 and caspase 9 protein expression in the testis of the SD group was highest among the three groups. In the epididymis, the expression of caspase 9 was significantly decreased in the LD group compared with the MD group ($p < .05$). Caspase 3 protein expression was increased in the SD and MD groups compared with the LD group ($p < .05$), and there was no significant difference between the SD and MD groups (Figure 9f,g).

LC3, P62, mTOR, and BECN1 expression levels were assessed by western blot analysis (Figure 10a).

The ratio of LC3II/LC3I represents autophagy levels in the testes; this ratio did not differ significantly between the three groups. P62 protein expression was higher in the LD group compared with the MD group ($p < .001$). However, in the epididymis, LC3 and P62 protein expression showed the opposite trend; LC3 protein expression was significantly increased, whereas P62 protein expression was significantly decreased in the SD and LD groups compared with the MD group ($p < .05$; Figure 10b,c). BECN1 and mTOR protein expression levels in the testes did not significantly differ among the three groups, whereas in the epididymis the expression of the two proteins decreased as follows: MD > SD > LD ($p < .05$; Figure 10d,e).

ATP synthase, CS, Drp1, Mff, and Fis1 protein expression levels were assessed by western blot analysis (Figure 11a).

ATP synthase and CS protein expression in the testes did not significantly differ among the three groups. However, in the

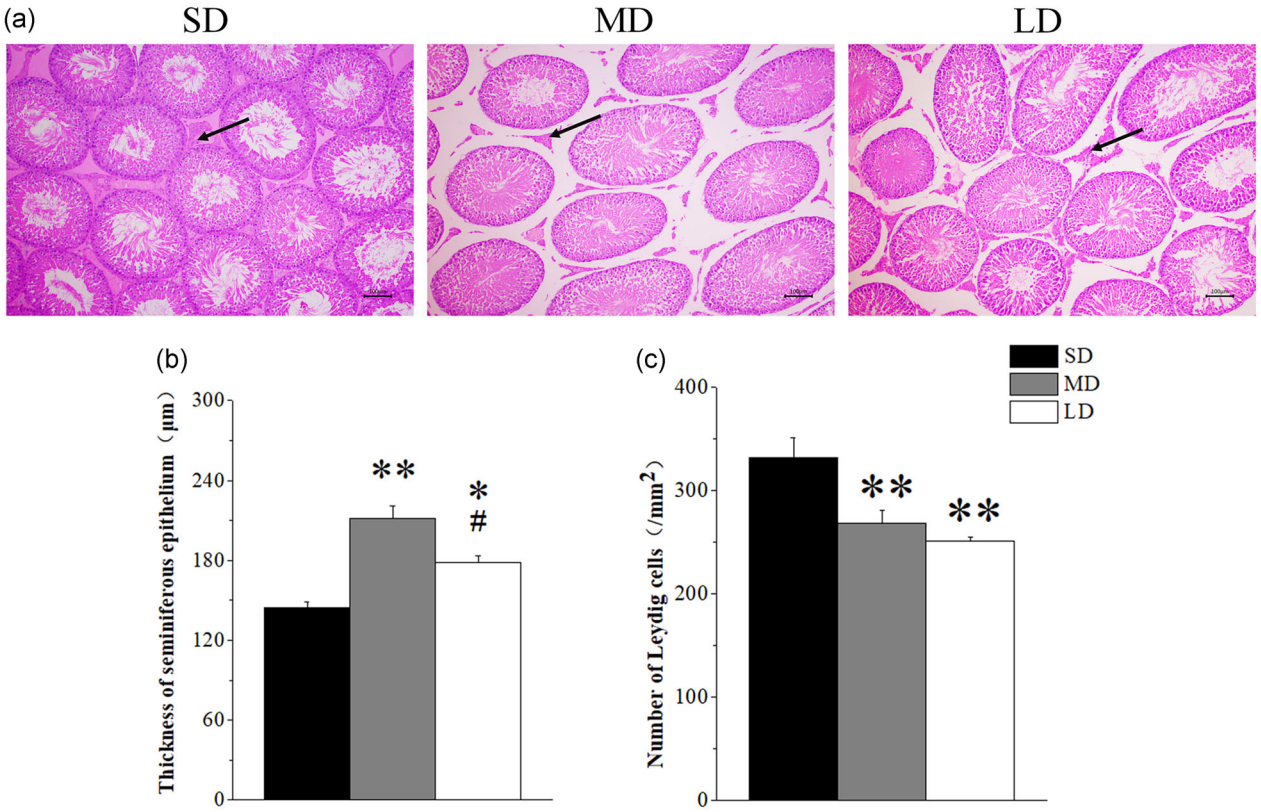

FIGURE 4 Changes in the thickness of the spermatogenic epithelia and Leydig cells of testis in hamsters from three photoperiodic groups with HE staining. (a) Seminiferous tubules in the testis of three photoperiods under low-power magnification. Arrow, Leydig cells. Scale bar = 100 μm. (b) The thickness of the spermatogenic epithelium in a single seminiferous tubule of testis in hamsters during three photoperiods. (c) The number of Leydig cells in a single seminiferous tubule of testis in hamsters during three photoperiods. $n = 10$. HE, hematoxylin and eosin; LD, long daylight; MD, moderate daylight; SD, short daylight. $^{*}p < .05$, $^{**}p < .01$, relative to SD; $^{\#}p < .05$ relative to MD

epididymis, the expression levels of both proteins were the lowest in the SD group ($p < .05$; Figure 11b,c). In the testes, Drp1 and Mff protein expression levels were the lowest in the MD group ($p < .01$), whereas Fis1 protein expression was the highest in the SD group ($p < .05$). In the epididymis, Drp1, Mff, and Fis1 protein expression levels were the highest in the MD group ($p < .05$; Figure 11d–f), in contrast to the observed changes in the testes (Figure 12).

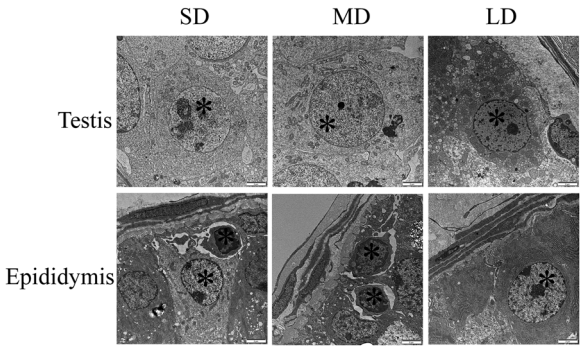

FIGURE 5 Nuclei ultrastructure of the testis and epididymis in hamsters under three photoperiod conditions. In the testes of the SD group and epididymides of the MD group, the nuclei (see arrow) of germ cells are deformed, and chromatin is condensed. Scale bar = 2 μm. LD, long daylight; MD, moderate daylight; SD, short daylight

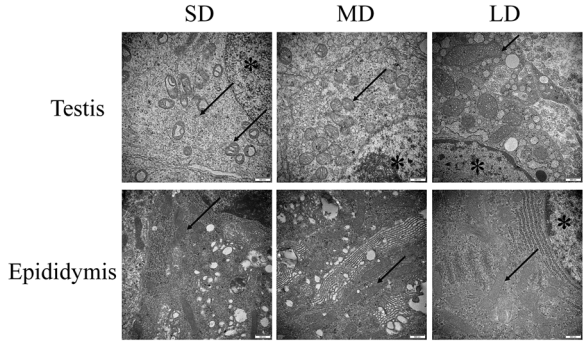

FIGURE 6 Cristae of mitochondria of the testes and epididymides of hamsters from three photoperiod groups. In the testes of the SD group, the mitochondria (see arrow) are in disarray. The mitochondria in the testes and epididymides of the other groups were normal, and the membranes are clear. There were no significant differences in mitochondrial morphology in the epididymides of the three groups. Scale bar = 500 nm. LD, long daylight; MD, moderate daylight; SD, short daylight

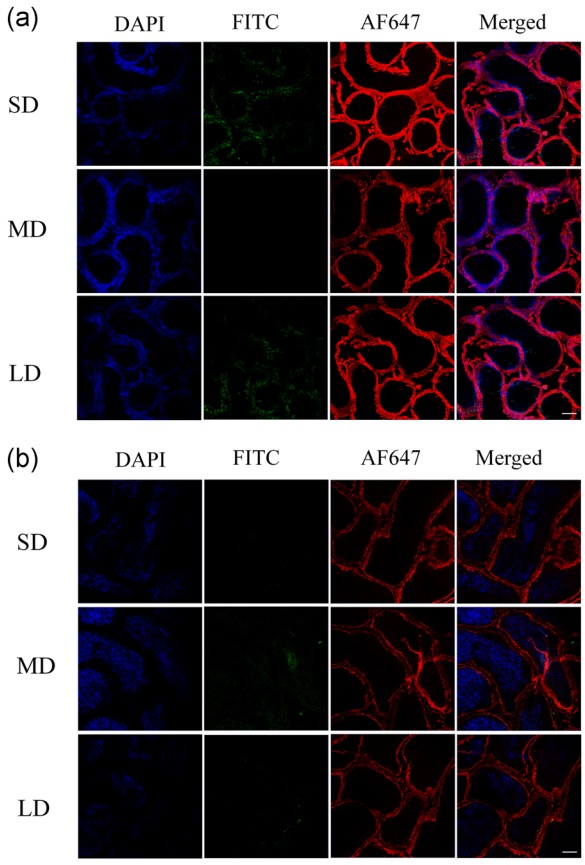

FIGURE 7 Fluorescent terminal deoxynucleotidyl transferase biotin-dUTP nick end-labeling (TUNEL) staining of testis and epididymis in hamsters from three photoperiod groups. (a) TUNEL staining of testis of hamsters from three photoperiodic groups. Scale bar = 100 μm. (b) TUNEL staining of epididymis of hamsters from three photoperiodic groups. Scale bar = 100 μm. Immunofluorescence histochemistry showing cell apoptosis, cell boundaries, and nuclei. Blue represents 4′,6-diamidino-2-phenylindole (DAPI)-stained nuclei; red represents Alexa Fluor 647-stained laminin of interstitial tissue, and the green represents TUNEL by FITC. LD, long daylight; MD, moderate daylight; SD, short daylight

4 | DISCUSSION

In this study, we used a variety of techniques to explore the morphological and functional changes and mechanisms of different sex organs of striped dwarf hamsters under different photoperiods from a multidimensional perspective. The results showed that SD conditions induced a reduction in weight and structural atrophy of the testes and epididymides in hamsters, whereas under LD conditions those organs remained unchanged or exhibited mild atrophy compared with MD conditions. The levels of testicular function-related hormones, such as FSH, LH, and TTE, in the LD group were lower than those in the MD and SD groups. In SD conditions, the apoptosis level in the testes increased, and autophagy levels remained stable, whereas in the epididymis, apoptosis levels remained the same and autophagy levels increased. The effects of apoptosis and autophagy may be the main causes of sexual organ degradation. Interestingly, mitochondrial fission levels increased in the testes and decreased in the epididymides under SD and LD conditions, and mitochondrial function remained stable in the testes and decreased in the epididymides, reflecting significant tissue differences.

After 8 weeks of photoperiod treatment, the body weights of the hamsters decreased under SD conditions compared with the control MD conditions, but there was no significant difference compared with that before treatment. These findings are similar to those of a previous study showing that the body weights of striped dwarf hamsters after 8 weeks of treatment under SD or LD did not significantly differ compared with those before treatment (D. L. Xu & Hu, 2017). On one hand, we speculate that different mammals may cause the insensitive to light and weight gain under short photoperiod treatment with a period time, such as Siberian hamsters or Chinese hamsters (*Cricetulus griseus*; Bartke & Parkening, 1981; Mauer & Bartness, 1994; Tups et al., 2006). On the other, SD conditions could inhibit body weight gain in small mammals such as Syrian and Siberian hamsters; results from previous studies showed that 12.5 hr or more of light could maintain gonadal activity or irritant recurrence, and 12 hr or less could induce gonad degeneration (Bartness & Wade, 1985; Elliott, Stetson, & Menaker, 1972; Gaston & Menaker, 1967; Gorman, 2003; Klingenspor, Niggemann, & Heldmaier, 2000). In this study, the body weights of hamsters in the SD group did not significantly differ from those before treatment, but they were significantly lower than in the MD control group; this may be partly related to the described effect.

One of the most important discoveries from this study is that the tissue structure and function of testis and epididymis degenerated to varying degrees compared with the MD under SD and LD conditions, as those photoperiods corresponded to the nonbreeding seasons. However, compared with MD conditions, the wet weight and TWW/CW of the testes and epididymides were significantly decreased under SD conditions, and the diameter of the seminiferous tubules of the testes, the thickness of spermatogenic epithelial, and the numbers of Sertoli cells and spermatogonia in a single tubule were markedly decreased, indicating weakening of male reproductive function by morphological changes in the testes and tissue atrophy in hamsters under SD conditions, that is, corresponding to the winter photoperiod. We also hypothesize that the decrease in the diameter of testicular seminiferous tubules and the thickness of seminiferous epithelia may be caused by the decrease in the numbers of Sertoli cells and spermatogonia. This is similar to studies with Syrian hamsters, Siberian hamsters, and marmots (*Prairie dog*) that observed losses of testicular weight and decreases in the number of Sertoli cells and the thickness of seminiferous epithelium under SD conditions (Bergmann, 1987; Hikim, Amador, Klemcke, Bartke, & Russell, 1989; Hikim et al., 1991). Similar to the seasonal variation in South American plains vizcacha (*Lagostomus maximus*), testicular weight decreases, the size of seminiferous tubules decreases, and the testicular structure undergoes atrophy during the nonreproductive northern hemisphere winters (González et al., 2018). It is worth noting that serum MT levels were the highest under SD conditions in this study. Based on the fact that the testes and seminal vesicle

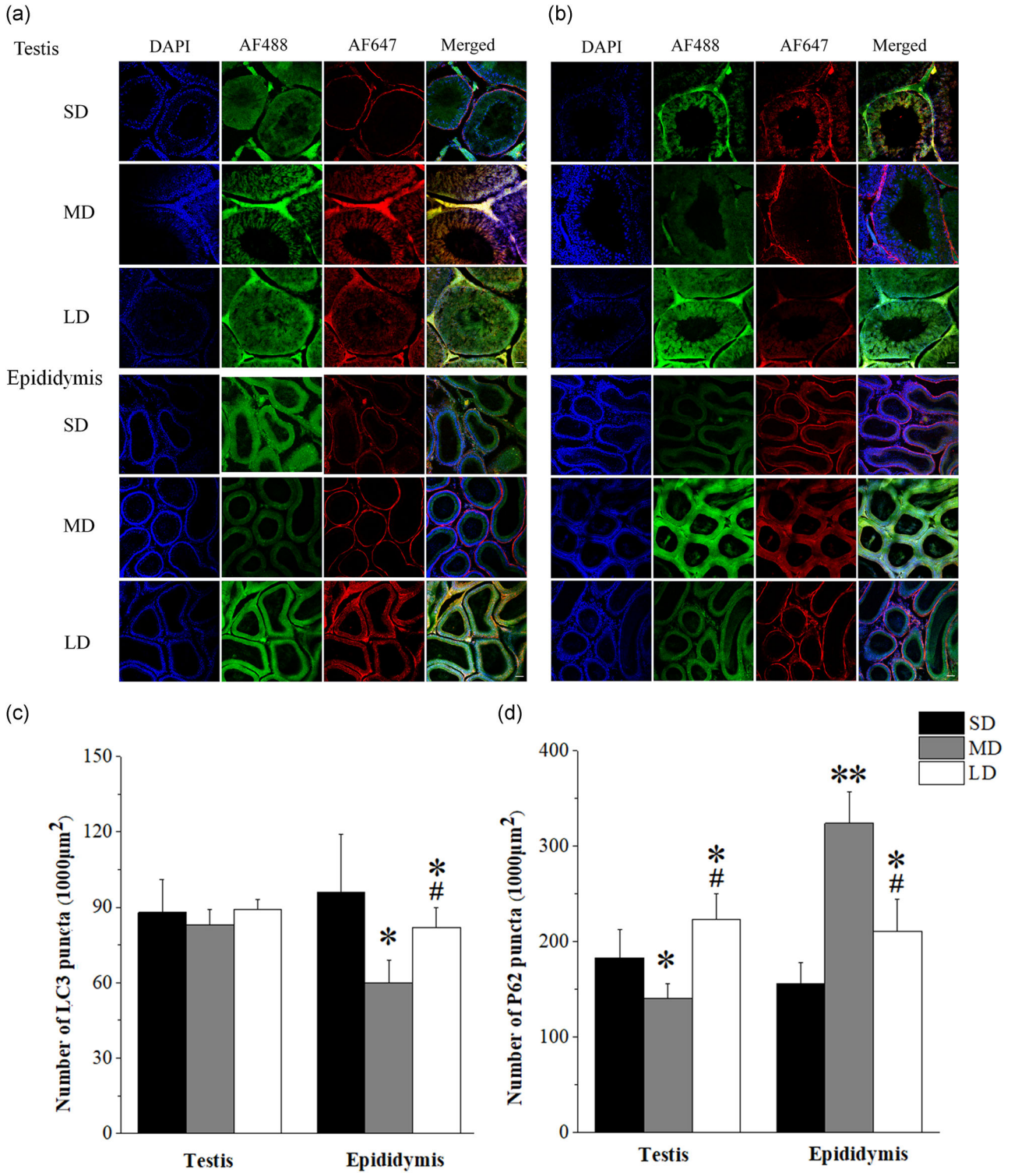

FIGURE 8 Quantification of LC3 and P62 puncta in the testis and epididymis of hamsters in three photoperiod groups. (a) Immunofluorescence histochemistry showing LC3 puncta of the testis and epididymis of hamsters. (b) Immunofluorescence histochemistry showing P62 puncta of the testis and epididymis of hamsters. Blue represents 4′,6-diamidino-2-phenylindole (DAPI)-stained nuclei; red represents Alexa Fluor 647-stained laminin of interstitial tissue, and the green represents AF488-stained LC3 or P62. Scale bar = 50 μm. (c) Quantification of LC3 puncta. Six images were analyzed in each sample; 10 samples were analyzed in each group. Values are the means ± standard deviation. LD, long daylight; MD, moderate daylight; SD, short daylight. $^{*}p < .05$, $^{**}p < .01$ compared with SD; $^{\#}p < .05$ relative to MD

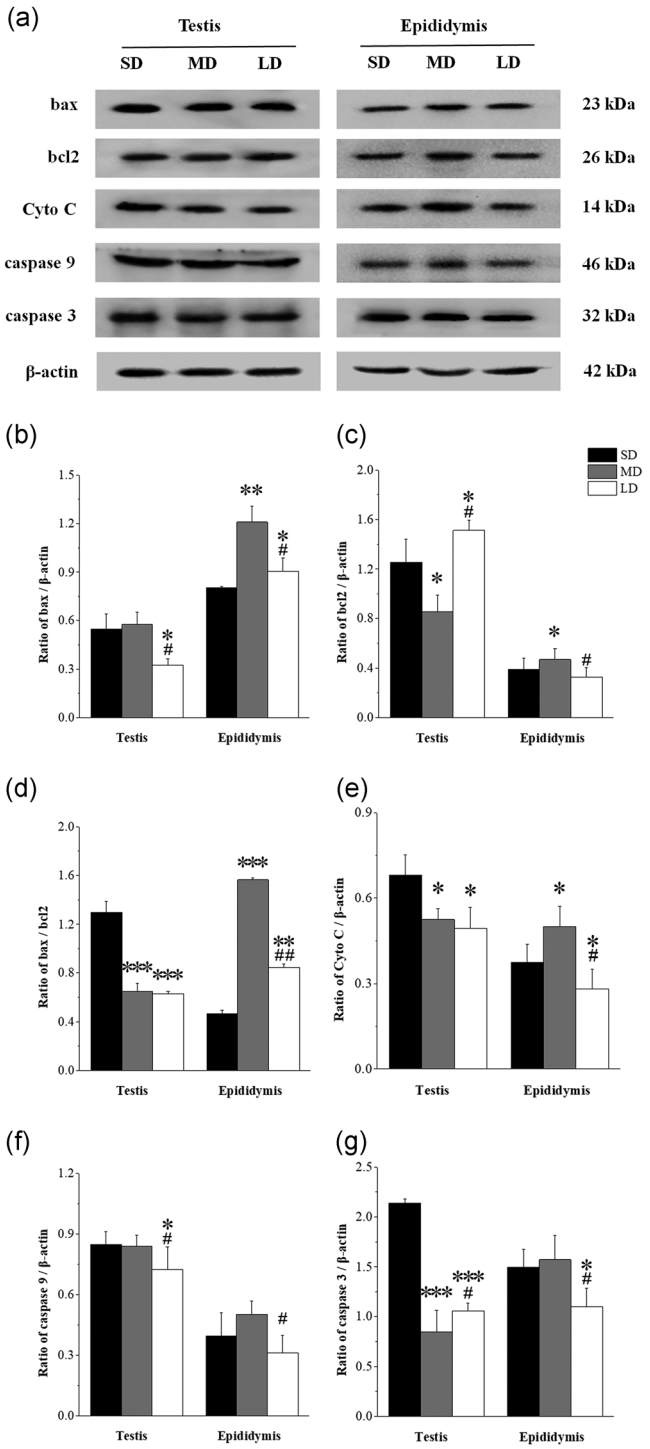

FIGURE 9 Expression of apoptosis-related proteins of the testis and epididymis in hamsters from three different photoperiod groups. (a) Representative immunoblots of bax, bcl2, Cyto *C*, caspase 9, caspase 3, and β-actin in three different photoperiod groups. (b) Ratio of bax to β-actin. (c) Ratio of bcl2 to β-actin. (d) Ratio of bax to bcl2. (e) Ratio of Cyto *C* to β-actin. (f) Ratio of caspase 9 to β-actin. (g) Ratio of caspase 3 to β-actin. Values are means ± standard deviation. $n = 10$. LD, long daylight; MD, moderate daylight; SD, short daylight. $^{*}p < .05$, $^{**}p < .01$, $^{***}p < .001$ relative to SD; $^{\#}p < .05$, $^{\#\#}p < .01$ relative to MD

weights and body weights of marsh rice rats (*Oryzomys palustris*) decreased after injecting melatonin (Edmonds, 2013), we hypothesize that the atrophy of testicular tissue structure under SD conditions may be related to the high serum MT levels. Although the wet weight of the testis and epididymis and TWW/CW, the diameter of testicular seminiferous tubules, and the number of Sertoli cells remained stable under LD conditions compared with the MD conditions, the number of spermatogonia in a single tubule and the thickness of seminiferous epithelium in the testis decreased, indicating the degeneration of structure in the testis to some extent. This prompted us to conclude that the tissue structure of testis under LD is better preserved than that under SD and is similar to that observed in Siberian hamsters, in which testicular weight after 15 and 30 weeks of LD treatment was significantly higher than that of SD (Bertoni, Sprenkle, Hanifin, Stetson, & Brainard, 1992; Duncan, 1994). However, the concentrations of serum FSH, LH, and fecal TTE decreased under LD conditions but remained stable under SD conditions compared with MD conditions. FSH, LH, and TTE are the main regulators of germ cell development by pulses release (Babu, Sadhnani, Swarna, Padmavathi, & Reddy, 2004; Chandrashekar, Majumdar, & Bartke, 1994); the decrease in serum or fecal concentrations under LD conditions may indicate the weakening of hamster reproductive ability. In view of the fact that TTE is mainly secreted by Leydig cells (Banihani, 2018), the increase in the number of Leydig cells under SD conditions may be one of the reasons why testosterone secretion remains unchanged despite the decrease in testicular weight. Generally, the atrophy of testicular tissue structure under SD conditions and the decrease in testicular-related hormone levels under LD may be one of the main reasons for the decline in male hamster reproductive ability in the short and long photoperiods corresponding to the two nonbreeding seasons.

LC3II is an autophagy effector and marker protein (Zhou et al., 2013), and P62 is an autophagy transporter that is inversely related to autophagy levels (Nakano, Oki, & Kusaka, 2017; Zhang et al., 2019). Interestingly, in this study, the number of LC3 puncta and the LC3II protein expression levels in the testes of hamsters did not differ significantly among the three groups, whereas the number of P62 puncta and the protein expression of P62 increased under LD conditions. As LC3 is the most important factor for measuring autophagy levels (Schaaf et al., 2016), these results suggest that autophagy levels in the testis are likely to remain stable under different photoperiods. BECN1 is one of the key factors promoting autophagy, while mTOR is one of the main inhibiting factors of autophagy. In this study, compared with the control MD group, the expression levels of BECN1 and mTOR in the testis remained the same under SD and LD conditions; this may indicate an important mechanism for maintaining the stability of testicular autophagy levels. Unlike the observed changes in autophagy in the testes, compared with MD, the number of LC3 puncta and the protein expression of LC3 in the epididymides increased under both SD and LD conditions, indicating that the autophagy levels in the epididymis increased under both SD and LD. Studies have shown that the level of autophagy in the epididymides

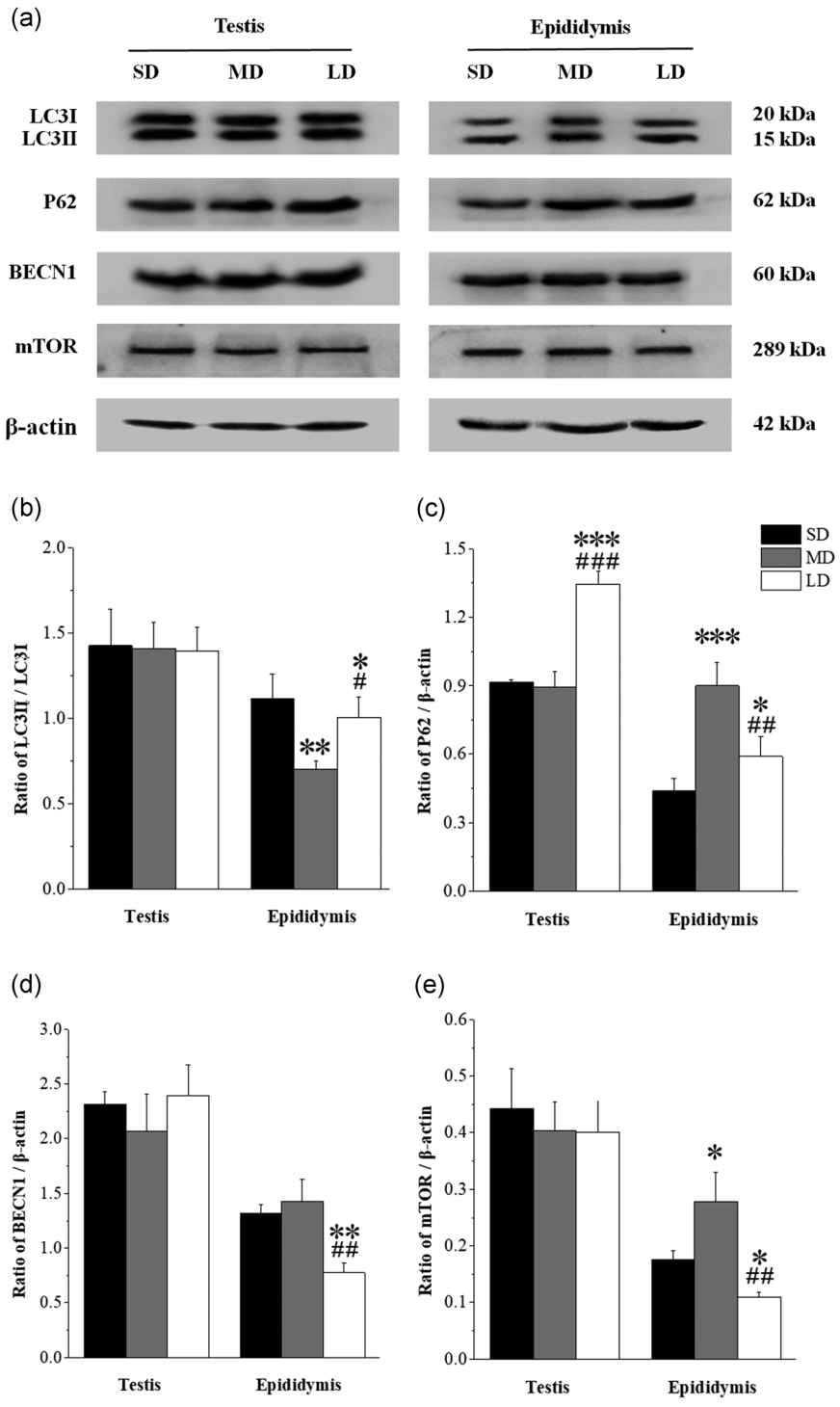

FIGURE 10 Expression of autophagy-related proteins of the testis and epididymis in hamsters of three different photoperiod groups. (a) Representative immunoblots of LC3I, LC3II, P62, BECN1, mTOR, and β-actin in three different photoperiodic groups. (b) Ratio of LC3II to LC3I. (c) Ratio of P62 to β-actin. (d) Ratio of BECN1 to β-actin. (e) Ratio of mTOR to β-actin. Values are the means ± standard deviation. $n = 10$. BECN1, beclin-1; LC3, light chain 3; LD, long daylight; MD, moderate daylight; mTOR, mammalian target of rapamycin; SD, short daylight. $^{*}p < .05$, $^{**}p < .01$, $^{***}p < .001$ relative to SD; $^{\#}p < .05$, $^{\#\#}p < .01$, $^{\#\#\#}p < .001$ relative to MD

of camels significantly increases in the winter under SD (Abdel-Maksoud, Hussein, & Attaai, 2019). The present study found similar results. In this study, BECN1 protein expression levels did not change under SD conditions, whereas mTOR decreased in the epididymis compared with MD conditions, indicating that the increase in autophagy levels in the epididymides may be mainly caused by a decrease in the inhibition of mTOR. The protein expression levels of BECN1 (46%, $p < .05$) and mTOR (61%, $p < .05$) decreased under LD conditions, indicating that the increase in epididymis autophagy levels under LD may be mainly mediated by a higher degree of downregulation of the inhibition of mTOR. In general, the autophagy levels in the testes were unchanged under both SD and LD conditions, whereas in the epididymides, the corresponding levels were increased, indicating tissue specificity.

We also found obvious DNA fragmentation in the testes, and ultrastructural assessment showed chromatin agglutination and

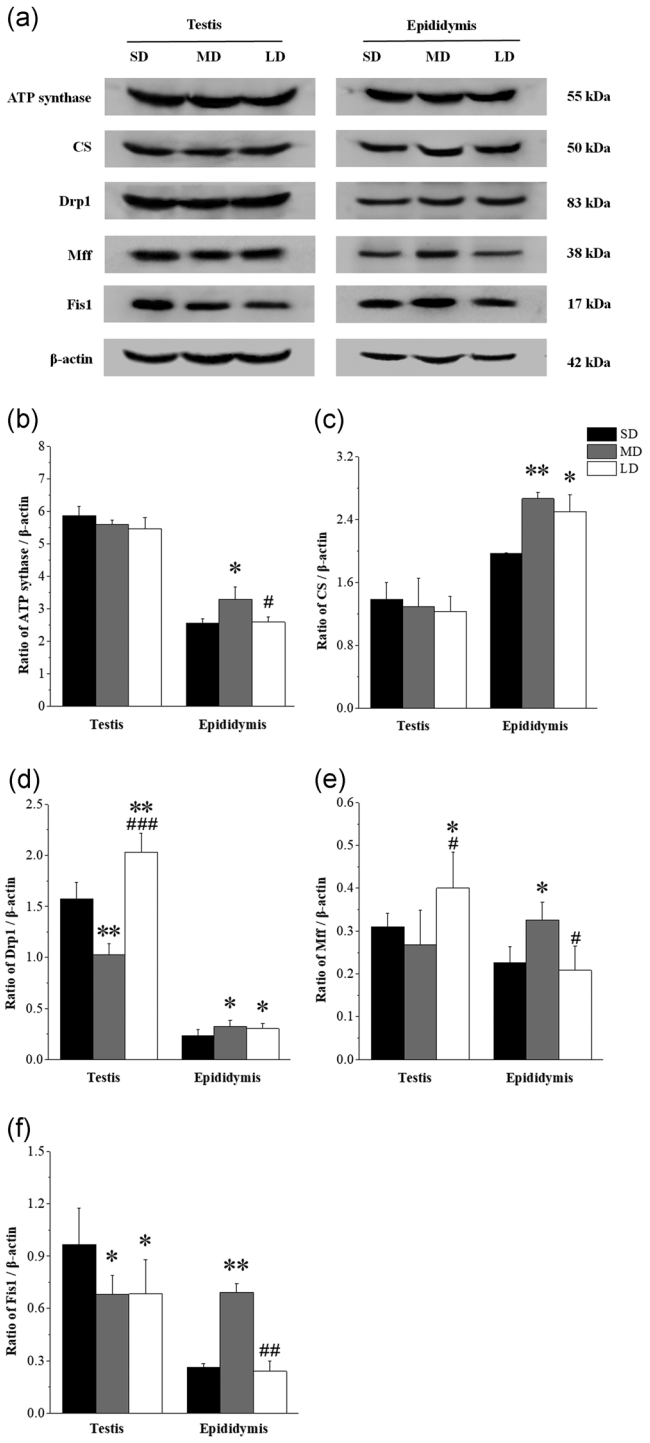

FIGURE 11 Expression of mitochondrial function-related proteins of the testis and epididymis of hamsters in three different photoperiod groups. (a) Representative immunoblots of ATP synthase, CS, Drp1, Mff, Fis1, and β-actin in three different photoperiod groups. (b) Ratio of ATP synthase to β-actin. (c) Ratio of CS to β-actin. (d) Ratio of Drp1 to β-actin. (e) Ratio of Mff to β-actin. (f) Ratio of Fis1 synthase to β-actin. Values are means ± standard deviation. $n = 10$. ATP, adenosine triphosphate; CS, citrate synthase; LD, long daylight; MD, moderate daylight; SD, short daylight. $^{*}p < .05$, $^{**}p < .01$ relative to SD; $^{\#}p < .05$, $^{\#\#}p < .01$, $^{\#\#\#}p < .001$ relative to MD

nuclear membrane contraction in the nuclei under SD conditions. As DNA fragmentation is one of the most important indicators of apoptosis, these results suggest the occurrence of apoptosis under these conditions. The ratio of bax to bcl2 is usually used to measure the level of mitochondrial apoptosis (Antonsson et al., 1997), whereas caspase 3 is a key enzyme in the execution and effect of nuclear apoptosis (Herr, 2018). In the testes, the protein expression levels of apoptosis-related factor bax/bcl2, Cyto *C*, caspase 9, and caspase 3 were increased in SD compared with MD conditions, indicating that the level of apoptosis caused by mitochondrial and nuclear apoptosis increased. The protein expression levels of bax/bcl2 and Cyto *C* in the testes were unchanged under LD conditions, suggesting that the level of apoptosis remained stable, whereas those in the epididymides decreased in both SD and LD conditions, indicating that the level of mitochondrial apoptosis decreased. The protein expression of caspase 3 was unchanged under SD, indicating that the level of nuclear apoptosis may be maintained in SD conditions. As studies have shown that increased apoptosis leads to loss of tissue weight (Furuta et al., 1994; Huang et al., 2016; Otsuka et al., 2010), the loss of testis weight in hamsters under SD exposure in this study may be related to the increase in apoptosis levels. This is similar to the findings in white-footed mice, Syrian hamsters, and bank voles, where the levels of testes apoptosis increased and testicular weight decreased under SD conditions (Bonda-Ostaszewska & Wlostowski, 2015; Morales et al., 2007; Young, Zirkin, & Nelson, 2001). In general, the loss of testis weight under SD may be caused by stable autophagy levels and increased apoptosis levels, while constant levels of autophagy and apoptosis may be one of the mechanisms of testicular quality maintenance under LD. The loss of epididymis weight under SD may be caused by an increase in autophagy levels and the maintenance of nuclear apoptosis levels, whereas an increase in autophagy levels and a decrease in apoptosis levels may be one of the mechanisms for maintaining epididymis weight under LD conditions.

Surprisingly, the protein expression levels of ATP synthase and CS in the testes showed no significant differences among the three photoperiods, although the level of apoptosis increased in the testes, suggesting that mitochondrial function did not change under different photoperiods. However, the expression levels of both proteins in epididymides decreased under both short and long daylight, suggesting that mitochondrial function weakened. The differences in mitochondrial function between testis and epididymis under different photoperiods may be related to changes in mitochondrial apoptosis and fission levels. Drp1 is the most important factor in mitochondrial fission; Mff promotes the activity of Drp1 (Mozdy, McCaffery, & Shaw, 2000), while Fis1 inhibits mitochondrial fission (Liu & Chan, 2015). In the testis, compared with MD, the ultrastructure under SD showed mitochondrial cristae damage, and the levels of bax/bcl2 and Drp1 increased, indicating that the levels of mitochondrial apoptosis and mitochondrial fission were significantly increased under SD. This suggests that the dynamic balance of

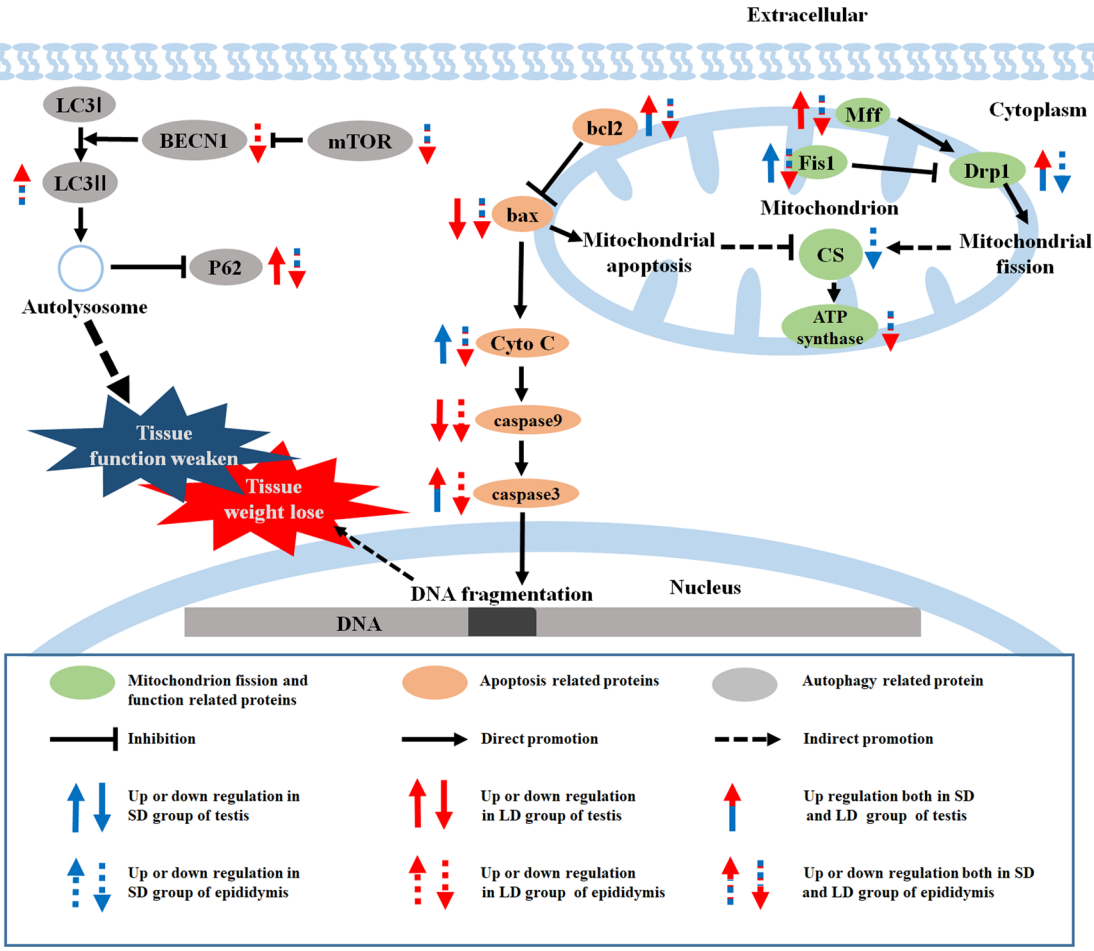

FIGURE 12 Graphical summary of the regulation of proteins. ATP synthase, adenosine triphosphate synthase; bax, bcl-2-associated X protein; bcl2, B cell lymphoma/leukemia-2; BECN1, beclin1; CS, citrate synthase; Cyto *C*, cytochrome *C*; Drp1, dynamin-related protein 1; Fis1, fission 1; LC3, microtubule-associated protein 1 light chain; Mff, mitochondrial fission factor; mTOR, mammalian target of rapamycin; P62, sequestosome 1

mitochondrial apoptosis and fission level maintains the stability of mitochondrial function under short daylight. In LD, mitochondrial fission levels increased, while mitochondrial apoptosis levels remained unchanged. The elevated levels of caspase 3 mean increased nuclear apoptosis levels, which may lead to impaired mitochondrial function throughout the tissue and may be one of the mechanisms by which the mitochondrial function of the testis remains stable under LD. In the epididymis, the protein levels of bax/bcl2 and Drp1 were decreased under SD and LD compared with MD, suggesting that the decrease in the levels of mitochondrial apoptosis and mitochondrial fission under SD and LD may have resulted in the decrease in mitochondrial function in the epididymis. In general, the levels of mitochondrial fission and apoptosis increase in the testes under either short or long daylight, this may lead to the maintenance of stable mitochondrial function, whereas the levels of mitochondrial fission decrease in the epididymides, which may be the main reason for the decrease in mitochondrial function.

In conclusion, we conducted a comprehensive study to explore the changes in and mechanisms of autophagy, apoptosis, mitochondria fission, and function in different sex organs of hamsters under various photoperiods. Our findings confirm that SD exposure can lead to the loss of weight and structural degradation of sexual organs, whereas LD exposure decreased testicular-related hormones, possibly leading to a weakening of the reproductive ability of male hamsters. The loss of sex organ weight under SD may be mainly caused by increases in apoptosis levels in the testes and autophagy levels in the epididymis. In addition, the stability of mitochondrial function in the testis and the decrease of the corresponding level in epididymis may be a molecular strategy for hamsters to protect testicular function under various photoperiods. In general, SD and LD exposure lead to weakened reproductive function of sexual organs in hamsters through different mechanisms that may involve the balance between apoptosis and autophagy, mainly by regulating mitochondrial fission levels to maintain mitochondrial function in the testis and epididymis.

ACKNOWLEDGMENTS

The National Natural Science Foundation of China (Nos. 31670385, 31770455, 31972283, and 31800308) supported this study. We

thank LetPub (www.letpub.com) for its linguistic assistance during the preparation of this manuscript.

CONFLICT OF INTERESTS

The authors declare that there are no conflict of interests.

AUTHOR CONTRIBUTIONS

Conceived and designed the research: L. X. X., J. H. X., Z. W. Performed the experiments: J. J. M., C. L. W., X. Q. Y., X. C. W. Analyzed the data and interpreted the results of experiments: J. J. M., Z. W. Prepared the figures: J. J. M. Drafted the manuscript: J. J. M., Z. W. Provided experimental guidance and suggestions for revision: J. H. X., Z. W., H. L. X., M. W., and L. X. X. Edited and approved the final version of the manuscript: J. J. M., J. H. X., Z. W.

DATA AVAILABILITY STATEMENT

The datasets used and/or analyzed during the current study are available from the corresponding author on reasonable request. Original images are included in the supplementary documents.

ORCID

Junjie Mou http://orcid.org/0000-0002-7598-6068
Jinhui Xu https://orcid.org/0000-0002-5550-1764
Zhe Wang https://orcid.org/0000-0002-4950-9954
Laixiang Xu https://orcid.org/0000-0002-6390-1653

REFERENCES

Abdel-Maksoud, F. M., Hussein, M. T., & Attaai, A. (2019). Seasonal variation of the intraepithelial gland in camel epididymis with special reference to autophagosome. *Microscopy and Microanalysis*, *25*(4), 1052–1060. https://doi.org/10.1017/s1431927619014557

Ansari, M., Zhandi, M., Kohram, H., Zaghari, M., Sadeghi, M., Gholami, M., … Benson, A. P. (2018). D-Aspartate amends reproductive performance of aged roosters by changing gene expression and testicular histology. *Reproduction, Fertility, and Development*, *30*(7), 1038–1048. https://doi.org/10.1071/rd17072

Antonsson, B., Conti, F., Ciavatta, A., Montessuit, S., Lewis, S., Martinou, I., … Martinou, J. C. (1997). Inhibition of Bax channel-forming activity by Bcl-2. *Science*, *277*(5324), 370–372.

Babu, S. R., Sadhnani, M. D., Swarna, M., Padmavathi, P., & Reddy, P. P. (2004). Evaluation of FSH, LH and testosterone levels in different subgroups of infertile males. *Indian Journal of Clinical Biochemistry*, *19*(1), 45–49. https://doi.org/10.1007/bf02872388

Banihani, S. A. (2018). Ginger and testosterone. *Biomolecules*, *8*(4), 119. https://doi.org/10.3390/biom8040119

Bartke, A., & Parkening, T. A. (1981). Effects of short photoperiod on pituitary and testicular function in the Chinese hamster, *Cricetulus griseus*. *Biology of Reproduction*, *25*(5), 958–962. https://doi.org/10.1095/biolreprod25.5.958

Bartness, T. J., & Wade, G. N. (1985). Photoperiodic control of seasonal body weight cycles in hamsters. *Neuroscience and Biobehavioral Reviews*, *9*(4), 599–612. https://doi.org/10.1016/0149-7634(85)90006-5

Bergmann, M. (1987). Photoperiod and testicular function in *Phodopus sungorus*. *Advances in Anatomy, Embryology and Cell Biology*, *105*, 1–76.

Bertoni, J. M., Sprenkle, P. M., Hanifin, J. P., Stetson, M. H., & Brainard, G. C. (1992). Effects of short photoperiod on ATPase activities in the testis of the immature Siberian hamster. *Biology of Reproduction*, *47*(4), 509–513. https://doi.org/10.1095/biolreprod47.4.509

Biazik, J., Vihinen, H., Anwar, T., Jokitalo, E., & Eskelinen, E. L. (2015). The versatile electron microscope: An ultrastructural overview of autophagy. *Methods*, *75*, 44–53. https://doi.org/10.1016/j.ymeth.2014.11.013

Bonda-Ostaszewska, E., & Wlostowski, T. (2015). Apoptosis, proliferation, and cell size in seasonal changes of body and organ weight in male bank voles *Myodes glareolus*. *Mammal Research*, *60*(3), 255–261. https://doi.org/10.1007/s13364-015-0224-2

Campbell, T. L., & Quadrilatero, J. (2016). Data on skeletal muscle apoptosis, autophagy, and morphology in mice treated with doxorubicin. *Data in Brief*, *7*, 786–793. https://doi.org/10.1016/j.dib.2016.03.009

Chandrashekar, V., Majumdar, S. S., & Bartke, A. (1994). Assessment of the role of follicle-stimulating hormone and prolactin in the control of testicular endocrine function in adult djungarian hamsters (Phodopus sungorus) exposed to either short or long photoperiod. *Biology of Reproduction*, *50*(1), 82–87. https://doi.org/10.1095/biolreprod50.1.82

Console, G. M., Jurado, S. B., Camihort, G., Calandra, R. S., Zitta, K., & Dumm, C. (2002). Morphological and biochemical changes of pituitary gonadotropes in male golden hamsters submitted to short and long photoperiods. *Cells Tissues Organs*, *171*(2-3), 177–187. https://doi.org/10.1159/000063711

Costa, D. S., Menezes, C. M. C., & Paula, T. A. R. (2007). Spermatogenesis in white-lipped peccaries (*Tayassu pecari*). *Animal Reproduction Science*, *98*(3-4), 322–334. https://doi.org/10.1016/j.anireprosci.2006.03.014

Danson, M. J., & Hough, D. W. (2001). Citrate synthase from hyperthermophilic Archaea. *Methods in Enzymology*, *331*, 3–12.

Duncan, M. J. (1994). Photoperiodic effects on puberty and specific 2-125I iodomelatonin binding sites in Siberian hamsters. *Brain Research*, *640*(1–2), 316–321. https://doi.org/10.1016/0006-8993(94)91887-2

Edmonds, K. E. (2013). Melatonin, but not auxin, affects postnatal reproductive development in the Marsh rice rat (*Oryzomys palustris*). *Zoological Science*, *30*(6), 439–445. https://doi.org/10.2108/zsj.30.439

Elliott, J. A., Stetson, M. H., & Menaker, M. (1972). Regulation of testis function in golden hamsters: A circadian clock measures photoperiodic time. *Science (New York, N.Y.)*, *178*(4062), 771–773. https://doi.org/10.1126/science.178.4062.771

Fekkes, P., Shepard, K. A., & Yaffe, M. P. (2000). Gag3p, an outer membrane protein required for fission of mitochondrial tubules. *Journal of Cell Biology*, *151*(2), 333–340.

Fu, W. W., Hu, H. X., Dang, K., Chang, H., Du, B., Wu, X., & Gao, Y. F. (2016). Remarkable preservation of Ca^{2+} homeostasis and inhibition of apoptosis contribute to anti-muscle atrophy effect in hibernating Daurian ground squirrels. *Scientific Reports*, *6*, 27020. https://doi.org/10.1038/Srep27020

Furuta, I., Porkka-Heiskanen, T., Scarbrough, K., Tapanainen, J., Turek, F. W., & Hsueh, A. J. (1994). Photoperiod regulates testis cell apoptosis in Djungarian hamsters. *Biology of Reproduction*, *51*(6), 1315–1321. https://doi.org/10.1095/biolreprod51.6.1315

Gaston, S., & Menaker, M. (1967). Photoperiodic control of hamster testis. *Science (New York, N.Y.)*, *158*(3803), 925–928. https://doi.org/10.1126/science.158.3803.925

González, C. R., Isla, M. L. M., & Vitullo, A. D. (2018). The balance between apoptosis and autophagy regulates testis regression and recrudescence in the seasonal-breeding South American plains vizcacha, *Lagostomus maximus*. *PLoS One*, *13*(1), e0191126. https://doi.org/10.1371/journal.pone.0191126

Gorman, M. R. (2003). Differential effects of multiple short day lengths on body weights of gonadectomized Siberian hamsters. *Physiological and Biochemical Zoology*, *76*(3), 398–405. https://doi.org/10.1086/374284

Han, Y. Y., Zhan, J. Q., Xu, Y., Zhang, F. W., Yuan, Z. R., & Weng, Q. (2017). Proliferation and apoptosis processes in the seasonal testicular development of the wild Daurian ground squirrel (Citellus dauricus Brandt, 1844). *Reproduction, Fertility, and Development*, *29*(9), 1680–1688. https://doi.org/10.1071/rd16063

Herr, A. B. (2018). Evolution of an allosteric "off switch" in apoptotic caspases. *Journal of Biological Chemistry*, *293*(15), 5462–5463. https://doi.org/10.1074/jbc.H118.002379

Hikim, A. P., Amador, A. G., Klemcke, H. G., Bartke, A., & Russell, L. D. (1989). Correlative morphology and endocrinology of Sertoli cells in hamster testes in active and inactive states of spermatogenesis. *Endocrinology*, *125*(4), 1829–1843. https://doi.org/10.1210/endo-125-4-1829

Hikim, A. P., Hikim, I. S., Amador, A. G., Bartke, A., Woolf, A., & Russell, L. D. (1991). Reinitiation of spermatogenesis by exogenous gonadotropins in a seasonal breeder, the woodchuck (*Marmota monax*), during gonadal inactivity. *The American Journal of Anatomy*, *192*(2), 194–213. https://doi.org/10.1002/aja.1001920208

Huang, W.-F., Zhang, C.-C., Liu, J., Song, L.-X., Peng, B., & Zhao, H.-X. (2016). Protective effect of Wuzi Yanzong prescription on apoptosis in germ cells of mice induced by cyclophosphamide. *Zhong yao cai = Zhongyaocai = Journal of Chinese Medicinal Materials*, *39*(5), 1143–1147.

Kawazu, S., Kishi, H., Saita, E., Jin, W. Z., Suzuki, A. K., Watanabe, G., & Taya, K. (2003). Inhibin secretion in the golden hamster (*Mesocricetus auratus*) testis during active and inactive states of spermatogenesis induced by the restriction of photoperiod. *Journal of Reproduction and Development*, *49*(1), 87–97.

Kelestimur, H., Ozcan, M., Kacar, E., Alcin, E., Yilmaz, B., & Ayar, A. (2012). Melatonin elicits protein kinase C-mediated calcium response in immortalized GT1-7 GnRH neurons. *Brain Research*, *1435*, 24–28. https://doi.org/10.1016/j.brainres.2011.11.040

Klingenspor, M., Niggemann, H., & Heldmaier, G. (2000). Modulation of leptin sensitivity by short photoperiod acclimation in the Djungarian hamster, *Phodopus sungorus*. *Journal of Comparative Physiology B, Biochemical, Systemic, and Environmental Physiology*, *170*(1), 37–43. https://doi.org/10.1007/s003600050005

Kramarova, T. V., Shabalina, I. G., Andersson, U., Westerberg, R., Carlberg, I., Houstek, J., … Cannon, B. (2008). Mitochondrial ATP synthase levels in brown adipose tissue are governed by the c-Fo subunit P1 isoform. *FASEB Journal*, *22*(1), 55–63. https://doi.org/10.1096/fj.07-8581com

Kus, I., Songur, A., Ozogul, C., Kavakli, A., Zararsiz, I., & Sarsilmaz, M. (2004). Effects of photoperiod on the ultrastructure of Leydig cells in rat. *Archives of Andrology*, *50*(3), 193–200. https://doi.org/10.1080/01485010490425476

Lewis, P. D. (2006). A review of lighting for broiler breeders. *British Poultry Science*, *47*(4), 393–404. https://doi.org/10.1080/00071660600829092

Liu, R., & Chan, D. C. (2015). The mitochondrial fission receptor Mff selectively recruits oligomerized Drp1. *Molecular Biology of the Cell*, *26*(24), 4466–4477. https://doi.org/10.1091/mbc.E15-08-0591

Manickam, P., Kaushik, A., Karunakaran, C., & Bhansali, S. (2017). Recent advances in cytochrome c biosensing technologies. *Biosensors and Bioelectronics*, *87*, 654–668. https://doi.org/10.1016/j.bios.2016.09.013

Mariño, G., Niso-Santano, M., Baehrecke, E. H., & Kroemer, G. (2014). Self-consumption: The interplay of autophagy and apoptosis. *Nature Reviews Molecular Cell Biology*, *15*(2), 81–94. https://doi.org/10.1038/nrm3735

Martinez-Hernandez, J., Seco-Rovira, V., Beltran-Frutos, E., Ferrer, C., Canteras, M., Sanchez-Huertas, M. D. M., & Pastor, L. M. (2018). Testicular histomorphometry and the proliferative and apoptotic activities of the seminiferous epithelium in Syrian hamster during spontaneous recrudescence after exposure to short photoperiod. *Reproduction in Domestic Animals*, *53*(5), 1041–1051. https://doi.org/10.1111/rda.13201

Mauer, M. M., & Bartness, T. J. (1994). Body fat regulation after partial lipectomy in Siberian hamsters is photoperiod dependent and fat pad specific. *The American Journal of Physiology*, *266*(3 Pt 2), R870–878.

Moore, W., Jr. (1965). Observations on the breeding and care of the Chinese Hamster, *Cricetulus griseus*. *Laboratory Animal Care*, *15*, 94–101.

Morales, E., Ferrer, C., Zuasti, A., Garcia-Borron, J. C., Canteras, M., & Pastor, L. M. (2007). Apoptosis and molecular pathways in the seminiferous epithelium of aged and photoinhibited Syrian hamsters (*Mesocricetus auratus*). *Journal of Andrology*, *28*(1), 123–135. https://doi.org/10.2164/jandrol.106.000778

Morales, E., Pastor, L. M., Ferrer, C., Zuasti, A., Pallares, J., Horn, R., … Canteras, M. (2002). Proliferation and apoptosis in the seminiferous epithelium of photoinhibited Syrian hamsters (*Mesocricetus auratus*). *International Journal of Andrology*, *25*(5), 281–287. https://doi.org/10.1046/j.1365-2605.2002.00363.x

Mozdy, A. D., McCaffery, J. M., & Shaw, J. M. (2000). Dnm1p GTPase-mediated mitochondrial fission is a multi-step process requiring the novel integral membrane component Fis1p. *Journal of Cell Biology*, *151*(2), 367–380.

Nakano, S., Oki, M., & Kusaka, H. (2017). The role of p62/SQSTM1 in sporadic inclusion body myositis. *Neuromuscular Disorders*, *27*(4), 363–369. https://doi.org/10.1016/j.nmd.2016.12.009

Otsuka, S., Namiki, Y., Ichii, O., Hashimoto, Y., Sasaki, N., Endoh, D., & Kon, Y. (2010). Analysis of factors decreasing testis weight in MRL mice. *Mammalian Genome*, *21*(3–4), 153–161. https://doi.org/10.1007/s00335-010-9251-0

Pieri, N. C. G., Santos, P. R. D., Roballo, K. C. S., Flamini, M. A., Barbeito, C. G., Ambrosio, C. E., … Martins, D. D. (2014). Seasonal variations cause morphological changes and altered spermatogenesis in the testes of viscacha (*Lagostomus maximus*). *Animal Reproduction Science*, *149*(3-4), 316–324. https://doi.org/10.1016/j.anireprosci.2014.07.007

Reznik, G., Reznik-Schuller, H., & Mohr, U. (1973). Comparative studies of organs in the European hamster (*Cricetus cricetus* L.), the Syrian golden hamster (*Mesocricetus auratus* W.) and the Chinese hamster (*Cricetulus griseus* M.). *Zeitschrift fur Versuchstierkunde*, *15*(5), 272–282.

Schaaf, M. B., Keulers, T. G., Vooijs, M. A., & Rouschop, K. M. (2016). LC3/GABARAP family proteins: Autophagy-(un)related functions. *FASEB Journal*, *30*(12), 3961–3978. https://doi.org/10.1096/fj.201600698R

Seco-Rovira, V., Beltran-Frutos, E., Ferrer, C., Saez, F. J., Madrid, J. F., & Pastor, L. M. (2014). The death of sertoli cells and the capacity to phagocytize elongated spermatids during testicular regression due to short photoperiod in Syrian hamster (*Mesocricetus auratus*). *Biology of Reproduction*, *90*(5), 10. https://doi.org/10.1095/biolreprod.113.112649

Shi, L., Li, N., Bo, L., & Xu, Z. (2013). Melatonin and hypothalamic-pituitary-gonadal axis. *Current Medicinal Chemistry*, *20*(15), 2017–2031. https://doi.org/10.2174/09298673113209990114

Tahka, K. M. (1988). Effect of differential photoperiod treatment on Leydig cell ultrastructure in the bank vole (*Clethrionomys glareolus* S.). *General and Comparative Endocrinology*, *71*(2), 318–330. https://doi.org/10.1016/0016-6480(88)90260-2

Tups, A., Barrett, P., Ross, A. W., Morgan, P. J., Klingenspor, M., & Mercer, J. G. (2006). The suppressor of cytokine signalling 3, SOCS3, may be one critical modulator of seasonal body weight changes in the Siberian hamster, *Phodopus sungorus*. *Journal of Neuroendocrinology*, *18*(2), 139–145. https://doi.org/10.1111/j.1365-2826.2005.01394.x

Turek, F. W., Elliott, J. A., Alvis, J. D., & Menaker, M. (1975). The interaction of castration and photoperiod in the regulation of hypophyseal and serum gonadotropin levels in male golden hamsters. *Endocrinology*, *96*(4), 854–860. https://doi.org/10.1210/endo-96-4-854

Wang, C., Zhang, R. M., Zhou, L., He, J. T., Huang, Q., Siyal, F. A., … Wang, T. (2017). Intrauterine growth retardation promotes fetal intestinal autophagy in rats via the mechanistic target of rapamycin pathway. *Journal of Reproduction and Development*, *63*(6), 547–554.

Wang, Z., Jiang, S. F., Cao, J., Liu, K., Xu, S. H., Arfat, Y., … Gao, Y. F. (2019). Novel findings on ultrastructural protection of skeletal muscle fibers during hibernation of Daurian ground squirrels: Mitochondria, nuclei, cytoskeleton, glycogen. *Journal of Cellular Physiology*, *234*, 13318–13331. https://doi.org/10.1002/jcp.28008

Wang, Z., Xu, J.-H., Mou, J.-J., Kong, X.-T., Wu, M., Xue, H.-L., & Xu, L.-X. (2020). Photoperiod affects harderian gland morphology and secretion in female *Cricetulus barabensis*: Autophagy. *Apoptosis, and Mitochondria. Frontiers in Physiology*, *11*, 408. https://doi.org/10.3389/fphys.2020.00408

Wang, Z., Xu, J.-H., Mou, J.-J., Kong, X.-T., Zou, J.-W., Xue, H.-l., … Xu, L.-X. (2020). Novel ultrastructural findings on cardiac mitochondria of huddling Brandt's voles in mild cold environment. *Comparative Biochemistry and Physiology Part A: Molecular & Integrative Physiology*, 110766. https://doi.org/10.1016/j.cbpa.2020.110766

Xu, D.-L., Hu, X.-K., & Tian, Y. (2018). Seasonal variations in cellular and humoral immunity in male striped hamsters (*Cricetulus barabensis*). *Biology Open*, *7*(12), bio038489. https://doi.org/10.1242/bio.038489

Xu, D.-L., & Hu, X.-K. (2017). Photoperiod and temperature differently affect immune function in striped hamsters (*Cricetulus barabensis*). *Comparative Biochemistry and Physiology A Molecular & Integrative Physiology*, *204*, 211–218. https://doi.org/10.1016/j.cbpa.2016.12.009

Xu, L., Xue, H., Li, S., Xu, J., & Chen, L. (2017). Seasonal differential expression of KiSS-1/GPR54 in the striped hamsters (*Cricetulus barabensis*) among different tissues. *Integrative Zoology*, *12*(3), 260–268. https://doi.org/10.1111/1749-4877.12223

Xue, H. L., Xu, J. H., Chen, L., & Xu, L. X. (2014). Genetic variation of the striped hamster (*Cricetulus barabensis*) and the impact of population density and environmental factors. *Zoological Studies*, *53*, 8. https://doi.org/10.1186/s40555-014-0063-x

Yang, C. X., He, Y., Gao, Y. F., Wang, H. P., & Goswami, N. (2014). Changes in calpains and calpastatin in the soleus muscle of Daurian ground squirrels during hibernation. *Comparative Biochemistry and Physiology Part A, Molecular & Integrative Physiology*, *176*, 26–31. https://doi.org/10.1016/j.cbpa.2014.05.022

Yerganian, G. (1958). The striped-back or Chinese hamster, *Cricetulus griseus*. *Journal of the National Cancer Institute*, *20*(4), 705–727.

Young, K. A., & Nelson, R. J. (2001). Mediation of seasonal testicular regression by apoptosis. *Reproduction*, *122*(5), 677–685. https://doi.org/10.1530/rep.0.1220677

Young, K. A., Zirkin, B. R., & Nelson, R. J. (2001). Testicular apoptosis is down-regulated during spontaneous recrudescence in white-footed mice (*Peromyscus leucopus*). *Journal of Biological Rhythms*, *16*(5), 479–488. https://doi.org/10.1177/074873001129002150

Zhang, Y., Guo, W., Chen, H., Gao, J. F., Xu, Z. P., Tao, L. M., … Xu, W. P. (2019). Spinetoram confers its cytotoxic effects by inducing AMPK/mTOR-mediated autophagy and oxidative DNA damage. *Ecotoxicology and Environmental Safety*, *183*, 9. https://doi.org/10.1016/j.ecoenv.2019.109480

Zhao, L., Zhong, M., Xue, H. L., Ding, J. S., Wang, S., Xu, J. H., … Xu, L. X. (2014). Effect of RFRP-3 on reproduction is sex- and developmental status-dependent in the striped hamster (*Cricetulus barabensis*). *Gene*, *547*(2), 273–279. https://doi.org/10.1016/j.gene.2014.06.054

Zhao, Z.-J., Cao, J.-M., Li, X.-L., & Yu, B. (2010). Seasonal variations in metabolism and thermoregulation in the striped hamster (*Cricetulus barabensis*). *Journal of Thermal Biology*, *35*(1), 52–57. https://doi.org/10.1016/j.jtherbio.2009.10.008

Zhou, L., Wang, H. F., Ren, H. G., Chen, D., Gao, F., Hu, Q. S., … Wang, G. H. (2013). Bcl-2-dependent upregulation of autophagy by sequestosome 1/p62 in vitro. *Acta Pharmacologica Sinica*, *34*(5), 651–656. https://doi.org/10.1038/aps.2013.12

SUPPORTING INFORMATION

Additional supporting information may be found online in the Supporting Information section.

How to cite this article: Mou J, Xu J, Wang Z, et al. Effects of photoperiod on morphology and function in testis and epididymis of *Cricetulus barabensis*. *J Cell Physiol*. 2020;1–17. https://doi.org/10.1002/jcp.29998